The analysis of tool vibration signals by Spectral Kurtosis and ICEEMDAN modes Energy for insert wear monitoring in turning operation

Mohamed Lamine BOUHALAIS (mouhamed_mars@hotmail.com)
Universite 8 Mai 1945 Guelma https://orcid.org/0000-0002-0944-0008
Mourad NOUIOUA
Universite 8 Mai 1945 Guelma

Research Article

Keywords: Wear monitoring, Turning, Vibration, Empirical decomposition, Spectral Kurtosis

Posted Date: April 2nd, 2021

DOI: https://doi.org/10.21203/rs.3.rs-357732/v1

The analysis of tool vibration signals by Spectral Kurtosis and ICEEMDAN modes Energy for insert wear monitoring in turning operation

° Mohamed Lamine BOUHALAIS[1] ° Mourad NOUIOUA[1]

[1] Mechanics Research Center. Po. Box 73B, 25021 Constantine, Algeria

Corresponding author E-mail : mouhamed_mars@hotmail.com

Abstract

Surface finish quality is becoming even more critical in modern manufacturing industry. In machining processes, surface roughness is directly linked to the cutting tool condition, a worn tool generally produces low quality surfaces, incurring additional costs in material and time. Therefore, tool wear monitoring is critical for a cost-effective production line. In this paper, the feasibility of a vibration-based approach for tool wear monitoring has been checked for turning process. AISI 1045 unalloyed carbon steel has been machined with TNMG carbide insert twenty-one times for a total of 27 minutes of machining, which was a necessary amount of time to exceed (300 μm) as a flank wear threshold. Vibration signals have been acquired during the operation and then processed in order to extract a correlation between the surface roughness, tool wear level and vibration comportment. First, Spectral kurtosis has been calculated for the twenty-one performed runs, the signals has then been decomposed with ICEEMDAN, the energy of the high frequency modes has been finally calculated. The Spectral Kurtosis has allowed the locating of the optimal frequency band that contains the machining vibration signature, yet it couldn't have been used for wear monitoring. On the other hand, the energy of optimal frequency ICEEMDAN modes has increased in direct proportion to the increase of surface roughness degradation and thus, to tool wear.

Keywords Wear monitoring, Turning, Vibration, Empirical decomposition, Spectral Kurtosis

Nomenclature

EMD	Empirical Mode Decomposition
EEMD	Ensemble Empirical Mode Decomposition
CEEMDAN	Complete Ensemble Empirical Mode Decomposition with Adaptive Noise
ICEEMDAN	Improved CEEMDAN
IMF	Intrinsic Mode Function
RMS	Root Mean Square
SNR	Signal-to-Noise Ratio
SK	Spectral Kurtosis
FFT	Fast Fourier Transform

Introduction

Machining processes are the core of the majority of manufacturing industries. The principle of machining is simple yet effective for high quality surface finish. Generally, a contact is made between a cutting tool and a workpiece in order to obtain a particular shape by material removal. However, this contact must be with specific parameters in order to get the desired results, namely, a surface roughness that is in accordance with the detailed workpiece specifications.

One of the parameters that may effect changes on workpiece surface condition is tool wear level. For example, the inserts used in turning process gradually loses their sharpness over time of machining, which creates thermo-mechanical phenomena that alters the surface finish of the workpiece [1]. Hence, the monitoring of the tool wear and the surface roughness is important. Signal processing has been used a lot for this purpose where several parameters including cutting force [2 - 4], temperature [5 - 9], current consumption [10], image processing [11], sound and vibration signals [1] [12 – 20], have been exploited for tool wear surveillance.

Vibration analyses are often favored due to their effectiveness when taking into account the small number of required instruments, the fast response time to wear level changes and the diversity of available tools [1]. In addition, Frequency domain features are usually preferred over time domain features because the latter may be sensitive to phenomena other than tool wear. However, Frequency domain features are difficult to extract because they are based on the right choice of the optimal frequency band. Therefore, a perfect approach would exploit the benefits of the two types, namely, a Time-Frequency approach.

One of the mostly proposed combinations between statistical indicators and Time-frequency tools in the previous works are with the wavelet analysis, in [21] the authors have used Discrete Wavelet Decomposition for grinding wheel wear monitoring, the RMS value and variance of the decomposed signals have been selected as features vector for feeding a support vector machine, the classification accuracy has reached 99 %. In another work [22], RMS and linear regression of wavelet transformed signals have been used to estimate tool wear in ramp cuts in end milling. In [23], high SNR frequency band has been extracted using derived wavelet frames, the spectrum of the chosen band has been then injected in a 2D Convolutional Neural Network that recognizes wear signs of milling tool during cutting operation. In [24], the authors predicted flank wear of a drilling tool with acceptable accuracy using wavelet packet transform.

Wavelet transform usually needs to be preconfigured to extract a particular feature, specifically, an appropriate Wavelet Mother must be preselected before the application, which is a major drawback for this type of analysis because the basis functions are fixed while the signals features may vary from case to case. Alternatively, the Empirical Mode Decomposition is a data-driven tool, able to do the same work of the Wavelet Analysis, which is the separation of the high-frequency components from the lower ones, without the need to set a basis decomposition function. In many works, EMD has been proven to be effective for tool wear monitoring, in [25] the authors have used the EMD for improving the sensitivity of the measured signals energy and mean power, and predict the tool wear for turning operation. In

[26] EMD has been used in order to eliminate the milling tool teeth frequency, the spindle speed components and isolate the milling process vibration signature for cutting conditions monitoring. In [27], turning acoustic signals have been decomposed with EMD and then analyzed by Hilbert-Huang Transform, a correlation between the sound pressure amplitude of the IMFs and the tool wear has been found. EMD has been combined with wavelet analysis in [28] in order to identify the different wear modes of a turning carbide tool. In another work [29] a Support vector machine has been fed with energy and energy entropy of IMFs obtained by EEMD and found to be effective for milling tool wear estimation, EEMD is an improved version of the original EMD decomposition proven to give better results in other applications [30 - 34].

In this paper, the statistical tool knows as Spectral Kurtosis, the ICEEMDAN which is a more improved version of the EMD and the energy scalar indicator, have been used together to monitor a carbide tool wear during the turning of unalloyed carbon steel. The workpiece has been machined twenty-one times for a total of 27 minutes in order to reach a wear level of more than 300 µm. The vibration signals have been captured during the operation. The insert wear and the surface roughness have been quantified after each run in order to check their correlation

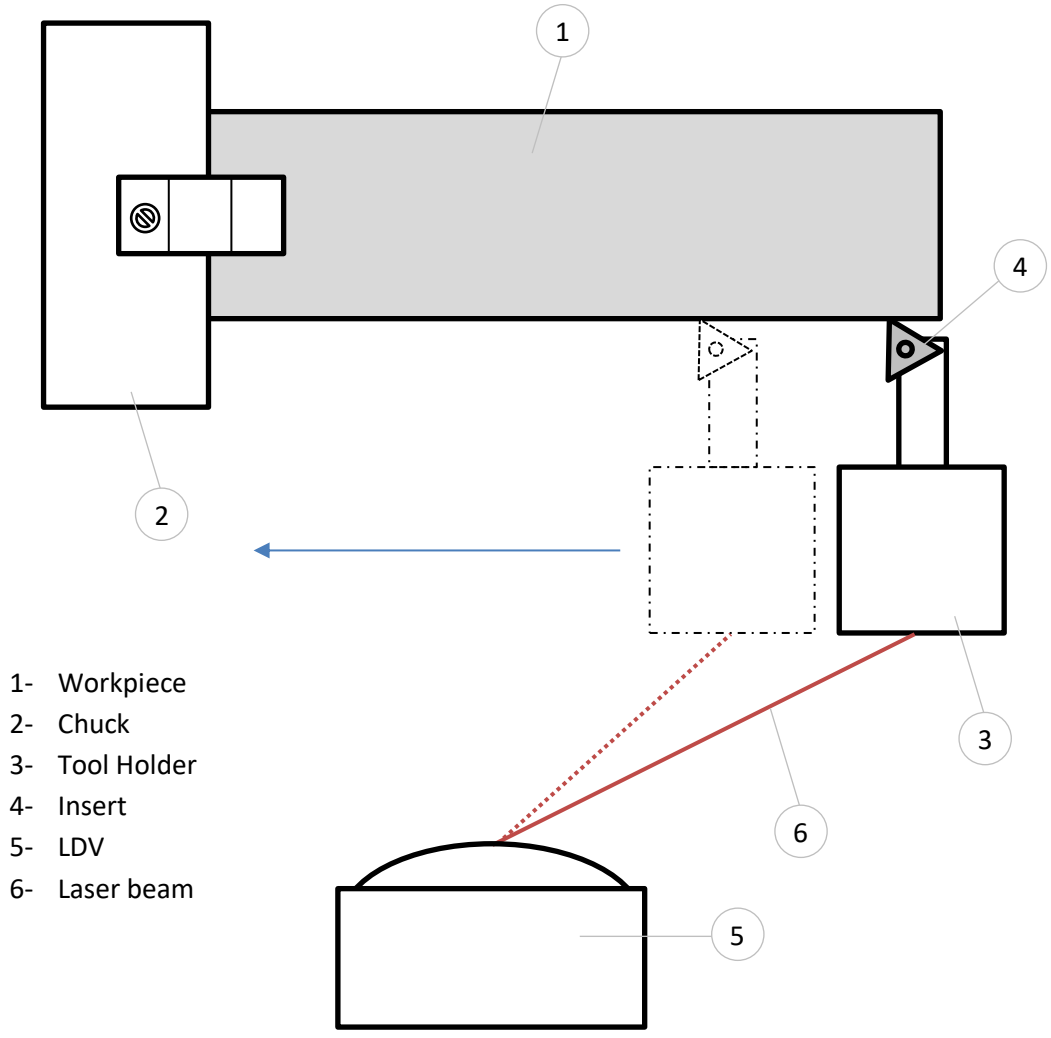

Fig. 1 The experimental setup

with the tool's vibration comportment. The feasibility of the proposed approach has been checked.

Experimental Setup

The tests have been conducted on a conventional KNUTH TURNADO lathe (**Fig. 2**), a workpiece of AISI 1045 unalloyed carbon steel that has the dimensions of (210 mm × 60 mm) has been machined with TNMG carbide insert. The machining conditions have been maintained as follows: V_c = 285m/min, f = 0.034 mm/Rev, a_p = 0.15 mm. Twenty-one runs have been carried out in order to reach the wear threshold (300 µm).

During each run, the cutting tool vibration signals have been acquired using an OPTOMET Scanning Laser Doppler Vibrometer. The laser beam has been focused on the tool holder end which has been covered with a reflective tape to enhance the laser signal. The vibrometer scanning speed has been set equal to the feeding speed so that the laser beam follows the tool holder (**Fig. 1**). Therefore, sixty acceleration signals have been captured in each run at different sections of the workpiece with a sampling frequency of 51200 Hz in the frequency band of (0 – 20000 Hz). The signals in question are presented in **Fig. 3**.

Run N°	Cumulated Machining time (s)	Surface roughness (µm)				Flank wear V_B (µm)
		Ra 1	Ra 2	Ra 3	Average	
1	76,8	0.8	0.845	0.8	0.815	50.078
2	153,6	0.74	0.7	0.7	0.713	119.078
3	230,4	0.91	0.73	0.73	0.790	127.234
4	307,2	1.46	1.5	1.06	0.340	135.4
5	384	1.2	1.105	1.6	1.302	148.911
6	460,8	1.39	1.105	1.59	1.62	161.992
7	537,6	0.94	1.14	0.72	0.933	171.818
8	614,4	0.82	0.76	0.7	0.760	180.751
9	691,2	0.705	0.845	0.72	0.757	184.9
10	768	1.195	1.33	1.43	1.318	193.082
11	844,8	1.155	1.21	1.29	1.218	202.9
12	921,6	0.82	0.882	1.34	1.014	206.179
13	998,4	1.77	1.42	1.76	1.650	220.905
14	1075,2	1.68	1.83	1.52	1.677	230.006
15	1152	2.46	2.2	2.17	2.277	232.353
16	1228,8	2.09	2.25	2.48	2.273	233.989
17	1305,6	2.64	1.86	2.74	2.413	237.284
18	1382,4	1.87	1.84	1.65	1.787	247.085
19	1459,2	2.189	1.93	2.189	2.103	250.357
20	1536	2.48	2.58	2.07	2.377	294.536
21	1612,8	1.55	1.69	1.7	1.647	320.594

Table. 1 The experimental data

At the end of each run, three values of surface roughness are measured with a PCE-RT 1200 2D Roughness tester. The cutting insert is then dismounted and placed in an OPTIKA metallographic microscope in order to measure the flank wear. The experimental data are shown in **Table 1**.

Fig. 2 The used equipments

Signal processing

For engine lathes, the raw vibration signal may contain gearbox meshing components, spindle rotational speed harmonics, cutting tool and workpiece natural frequencies, components of other rotating parts such as the feed rod and the bearings, plus some random components often described as noise. The isolation of the machining process vibration signature is necessary for a correct correlation between tool wear, tool vibration and surface roughness. For this step, the study proposes the use of ICEEMDAN as a decomposition algorithm that extracts the different vibration modes embedded in the whole captured signal.

ICEEMDAN is the improved version of the previous CEEMDAN algorithm, proven in many works to give better results when used in signal processing field. For the decomposition of a given signal $x(t)$ with CEEMDAN, the below steps are followed:

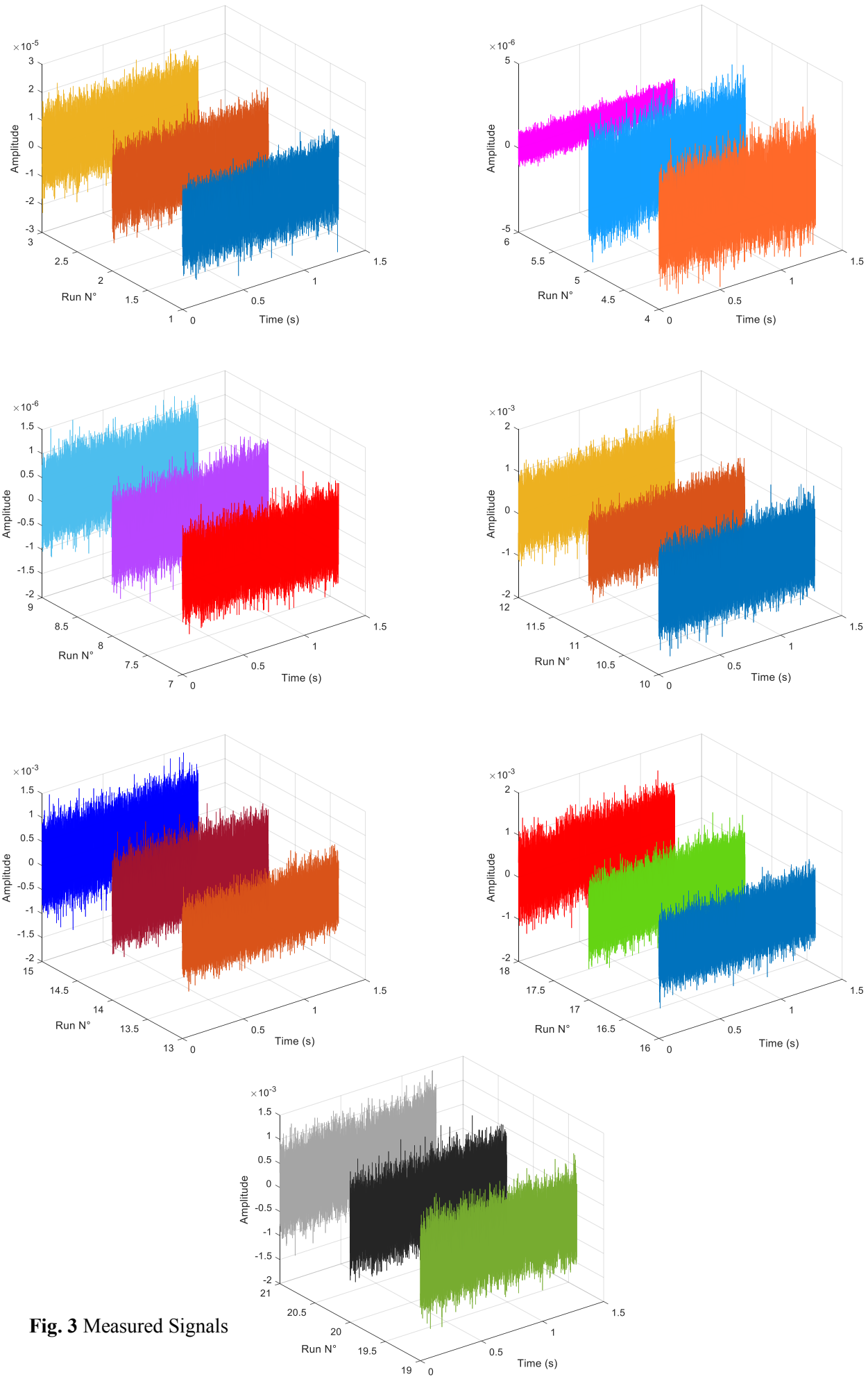

Fig. 3 Measured Signals

1. Decompose I realizations of $x(t) + \varepsilon_0 n^i(t)$ by EMD to obtain the first $\overline{IMF_1}$ by averaging:

$$\overline{IMF_1(t)} = \frac{1}{I}\sum_{i=1}^{I} IMF_1^i(t)$$

ε_0 is the signal-to-noise ratio.

n^i is the Gaussian white noise.

2. Calculate the first residue as:

$$r_1(t) = x(t) - \overline{IMF_1(t)}$$

3. Decompose I realizations of $r_1(t) + \varepsilon_1 E_1(n^i(t))$ until their first EMD mode and calculate the second mode:

$$\overline{IMF_2(t)} = \frac{1}{I}\sum_{i=1}^{I} E_1(r_1(t) + \varepsilon_1 E_1(n^i(t)))$$

Where E_j is an operator that produces the j^{th} mode obtained by EMD.

4. For $k = 2 \ldots . K$, calculate the k-th residue:

$$r_k(t) = r_{k-1}(t) - \overline{IMF_k(t)}$$

5. For $k = 2 \ldots . K$, define the $(k+1)$-th mode as:

$$\overline{IMF_{k+1}(t)} = \frac{1}{I}\sum_{i=1}^{I} E_1(r_k(t) + \varepsilon_k E_k(n^i(t)))$$

6. Go for step 4 for next k

Steps from 4 to 6 are repeated until the obtained residue in no longer feasible to be decomposed and satisfies:

$$R(t) = x(t) - \sum_{k=1}^{K} \overline{IMF_k}(t)$$

With K the total number of modes. The original signal $x(t)$ can be expressed in the end as:

$$x(t) = \sum_{k=1}^{K} \overline{IMF_k}(t) + R(t)$$

The ICEEMDAN algorithm follows instead these steps:

1- Calculate the upper and lower envelopes mean of I realizations $x^i(t) = x + \varepsilon_0 E_1 n^i(t)$ using the EMD algorithm.

2- Obtain the first residue r_1 by averaging the results of the first step:

$$r_1 = \langle M(x^i) \rangle$$

3- Calculate the first mode:

$$IMF_1 = x - r_1$$

4- Estimate the second residue r_2 as the average of upper and lower envelopes of the realizations $r_1 + \varepsilon_1 E_2\, n^i(t)$ and then calculate the second mode:

$$IMF_2 = r_1 - r_2$$

5- For $k = 3 \ldots . K$, calculate the k-th residue:

$$r_k = \langle M(r_{k-1} - \varepsilon_{k-1} E_k\, n^i(t)) \rangle$$

6- For $k = 3 \ldots . K$, define the kth mode as:

$$IMF_k = r_{k-1} - r_k$$

7- Go to step 4 for the next k

Spectral Kurtosis

Spectral kurtosis (SK) is a statistical tool that can locate non-stationary or non-Gaussian comportment in the frequency spectrum of a raw signal. SK can be used as a preprocessing tool that provide useful information such as filtering parameters. The spectral kurtosis *K(f)*, of a signal *s(t)* is calculated as follow:

$$K(f) = \frac{\langle |S(t,f)^4| \rangle}{\langle |S(t,f)|^2 \rangle^2} - 2, \quad f \neq 0$$

S(t, f) is the Short-time Fourier Transform of the signal *s(t)*

Wear quantification

In order to measure the flank wear, the cutting insert is dismounted after each run and then put under a metallographic microscope that enables the quantification of wear through the counting of the corresponding pixels in the image taken by the microscope high-resolution digital camera. **Fig. 4** shows the processed insert images of the twenty-one runs with their corresponding flank wear value.

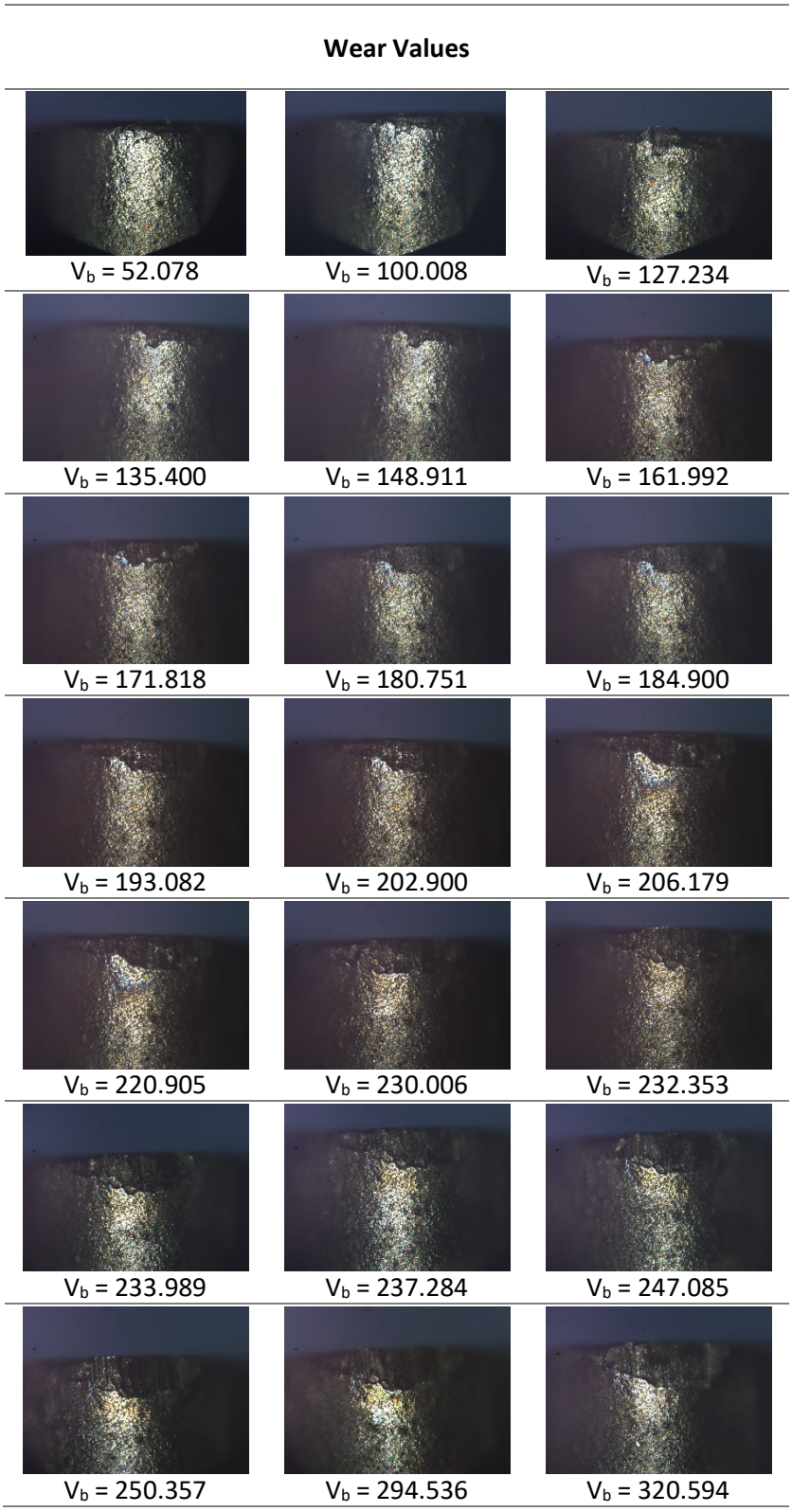

Fig. 4 Flank wear progression as shown by the microscope

Results and Discussion

Cutting inserts generally wear in a progressive manner. The speed of wear depends on several factors such as cutting parameters, workpiece material and the material of the cutting insert itself. The wear level is considered acceptable if the cutting edge keeps providing satisfactory results taking into account the specific parameters of surface roughness. After a certain wear level, which is generally above 300 µm, the surface roughness drastically degrades affecting the vibratory signature of the whole machining process. Therefore, surface condition and insert's wear level could be revealed by the surveillance of the vibration signals spectral composition.

Fig. 5 shows the FFT spectrums of the twenty-one captured signals. The examination of the spectral composition shows that the frequency band of [0 – 5000 Hz] has almost had the same frequency components over the whole twenty-one runs. Hence, the frequency peaks in this band cannot be linked to the surface condition, nor to the insert wear level. This has been confirmed with a contactless test, where we have turned on the lathe, activated the feeding movement with no contact between the cutting tool and the workpiece, and then captured the vibration signature. **Fig. 6** represents the signal spectrum of the band [0 – 8000 Hz], where we clearly notice the same frequency composition.

On the other hand, the components of the [5000 – 20000 Hz] band have behaved differently over the twenty-one tests. In the first three runs, equidistant peaks have clearly appeared between 10000 Hz and 20000 Hz, however, in the 4^{th}, 5^{th}, 6^{th}, 7^{th}, 8^{th} and 9^{th} runs, these peaks have been faded by the rising neighbor frequencies. The peaks reappear again in the runs [10^{th} – 17^{th}] with less clearness when compared to the first three runs. Finally, the followed frequency components are covered again in the last four runs spectrums. These fluctuations in the peaks level have been linked to the surface roughness variations.

In order to confirm this hypothesis, Spectral Kurtosis has been calculated for each run. **Fig. 7** shows the SK variation of the first three runs. A high SK value is noticed around 16 KHz, a synonym of the presence of non-gaussian behavior at the mentioned frequency. Notice that 16 KHz is included in the suspected frequency band. In addition, the SK value has slightly increased over the three performed runs, (1.47), (1.9) and (2.09) respectively, this might be related to insert wear increase. However, for the next runs, SK has stopped giving meaningful information, **Fig. 8** illustrates the SK non-regular variation of the fourth and fifth runs, from which it is very difficult to know where the non-gaussian components are concentrated in the frequency spectrum as we did previously. We mention that this behavior has been observed over eight runs, from the 4^{th} to the 11^{th} run, after that the highest SK value of the twelfth run has been around 16 KHz again (**Fig. 9**), yet its level has decreased to the value of (1.1). Once more, the SK has been irregular over the rest of runs, the twenty-first run is illustrated in **Fig. 10** as an example.

In another procedure, ICEEMDAN has been used to filter out the insignificant frequencies, namely the low frequency modes. The first modes produced by the ICEEMDAN decomposition contains generally the highest frequencies imbedded in the original signal,

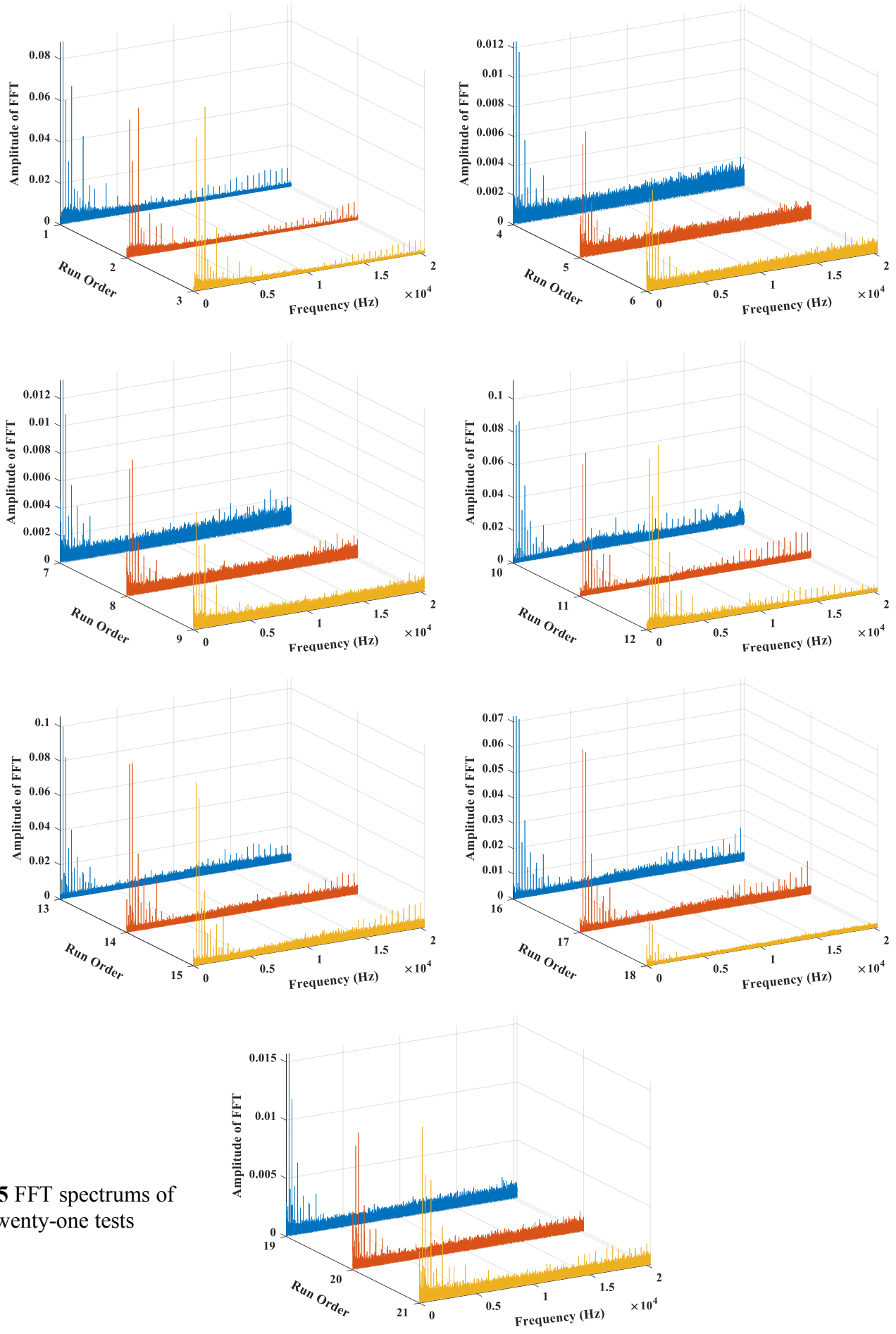

Fig. 5 FFT spectrums of the twenty-one tests

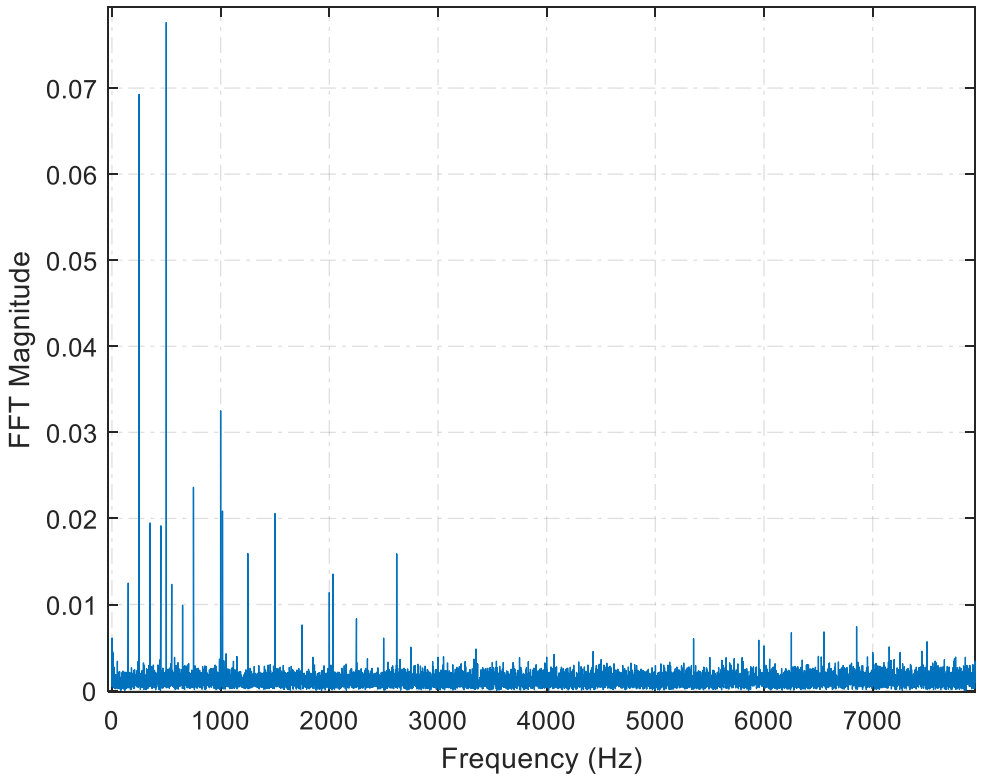

Fig. 6 Contactless Test signal spectrum

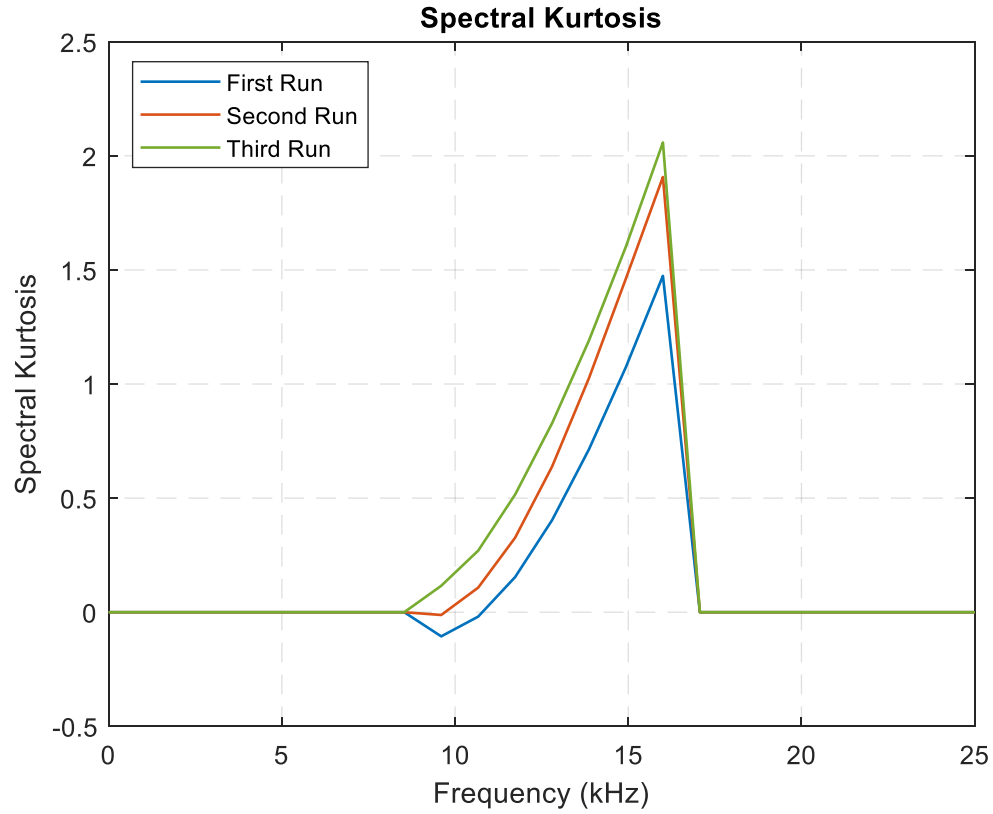

Fig. 7 SK of the first three runs signals

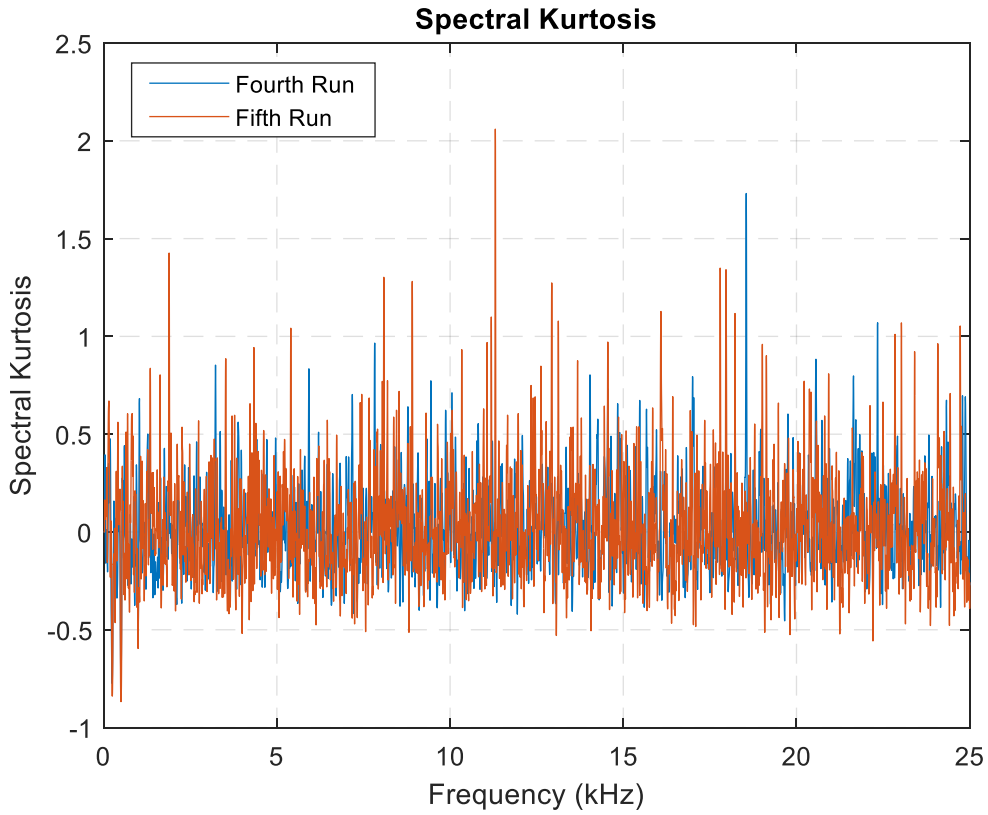

Fig. 8 Spectral Kurtosis of the Fourth and Fifth runs signals

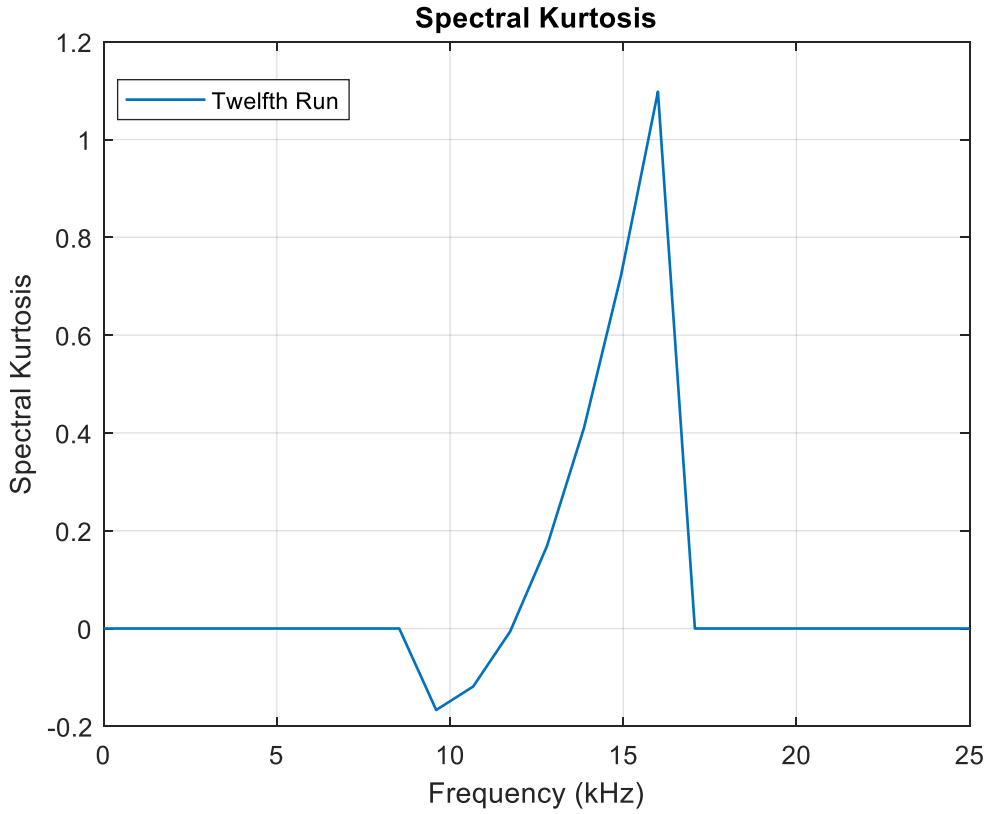

Fig. 9 Spectral Kurtosis of the Twelfth run signal

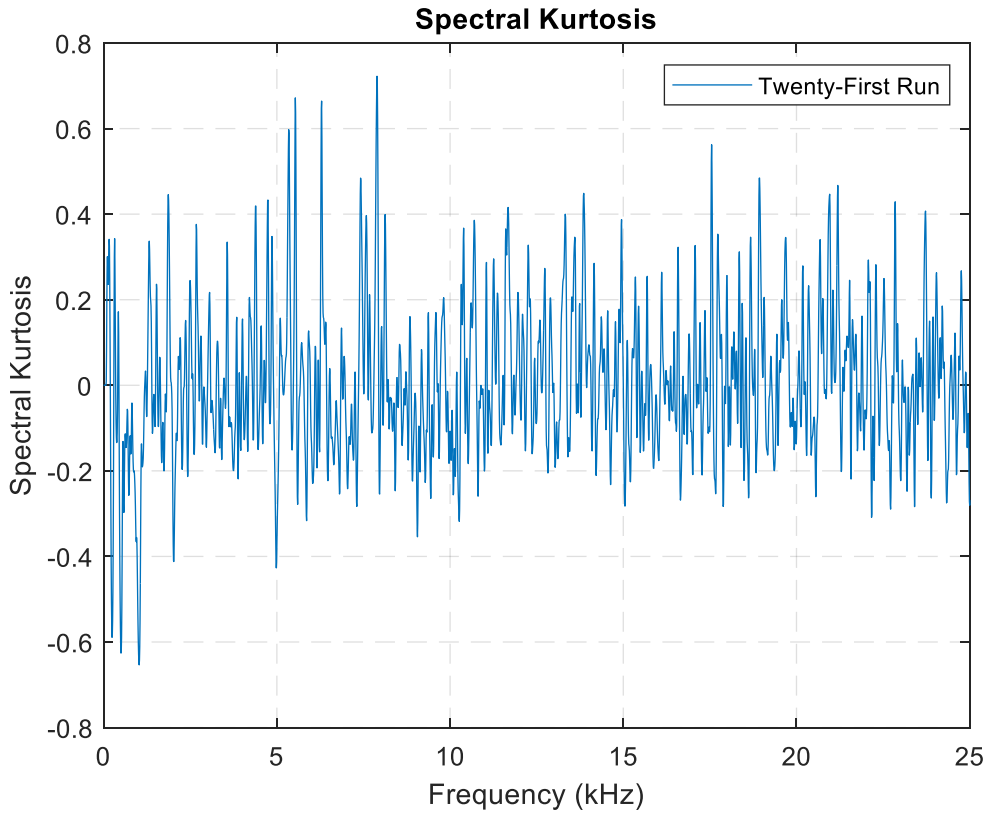

Fig. 10 Spectral Kurtosis of the Twenty-first run signal

which is in our case, the modes that perfectly covers the [5000 – 20000 Hz] band. Therefore, the energy of the first four IMFs of each captured signal has been calculated in order to follow the variations of the band magnitude. **Fig. 11** illustrates how the energy of the first four modes clearly increased after the 9th run with the same manner.

Furthermore, the investigation of the surface roughness variation during the twenty-one tests shows that *Ra* mean values have obviously increased after the 9th test as illustrated in **Fig. 12**. Thus, the augmentation of the IMFs energy could be correlated with the surface roughness increase.

Finally, the analysis of the tool wear behavior could explain the variations of the surface condition throughout the performed runs. The insert wear level has been gradually increasing as shown in **Fig.13**, the changes in the insert's edge shape are the main cause of surface condition degradations in our case, since machining parameters have been fixed.

Conclusion

This paper checked the feasibility of tool wear and surface roughness monitoring based on vibration analysis. A Laser Doppler Vibrometer has been used in order to acquire tool's vibration signals during the turning of unalloyed carbon steel. First, a contactless test has been performed to identify the lathes fundamental frequencies. Spectral Kurtosis has been then calculated for twenty-one runs vibration signals, which allowed to locate irregular behavior on

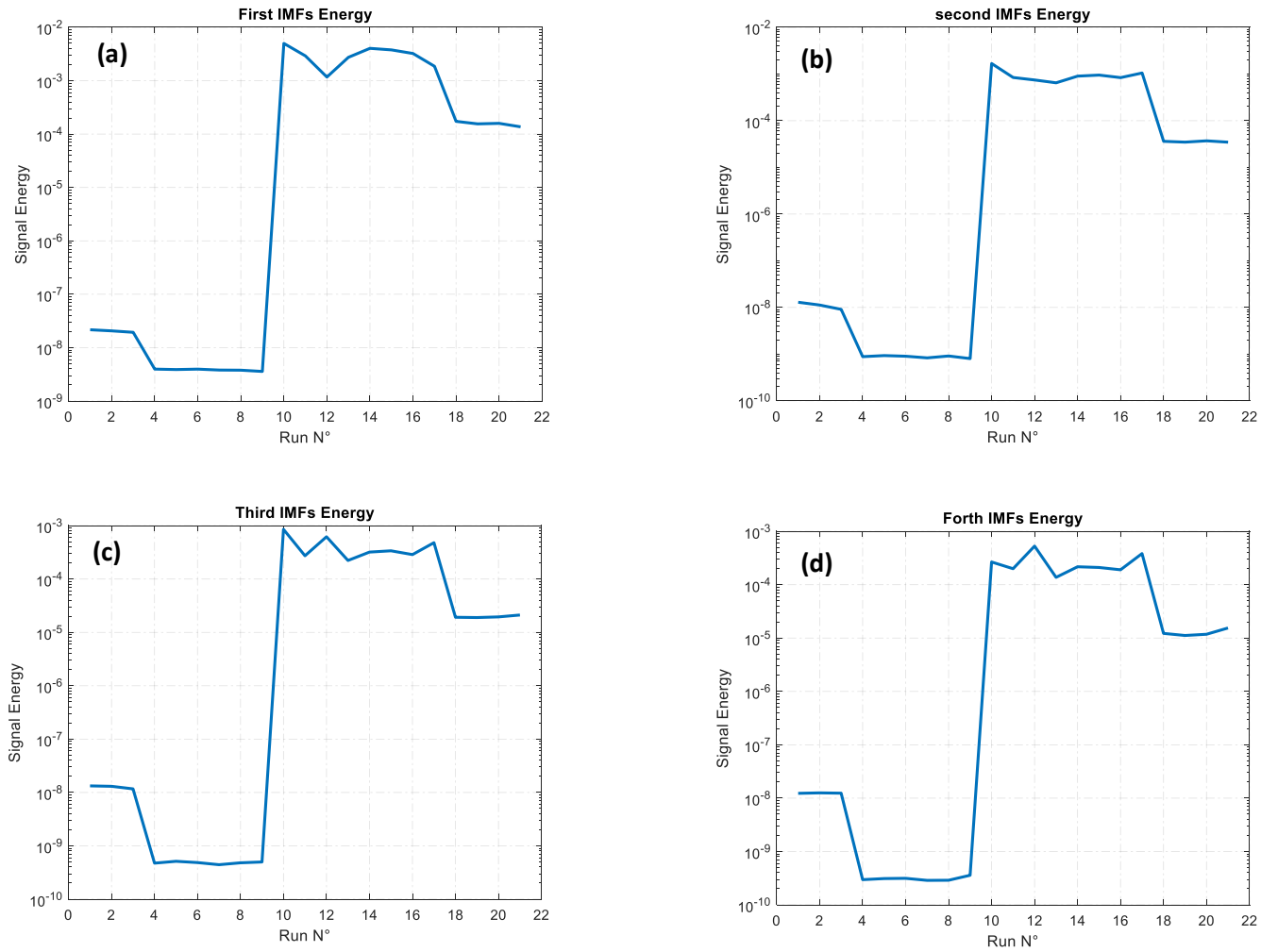

Fig. 11 IMF Energy variation over the twenty-one runs: Firsts (a), Seconds (b), Thirds (c) and Fourths (d)

the frequency spectrum. An empirical decomposition has been then performed using ICEEMDAN in order to isolate the significant vibration components from the lathe's frequencies. The analysis of the raw signals and their isolated modes with energy and Spectral Kurtosis variation has highlighted a correlation between the surface roughness, insert wear and tool's vibration comportment:

- SK has allowed to pinpoint the right frequency band linked to machining process, yet SK level variation is difficult to exploit for tool wear monitoring.
- The high frequency modes energy has increased in direct proportion to the increase of surface roughness.
- Insert wear has gradually increased and been the main cause of surface degradation in our case, where machining parameters has been fixed.
- Hight frequency vibration components energy can be used for tool wear and surface roughness monitoring.
- On the base of the SK analysis, only one IMF's energy has to be calculated in future, namely the IMF that covers the band that has the highest SK value.

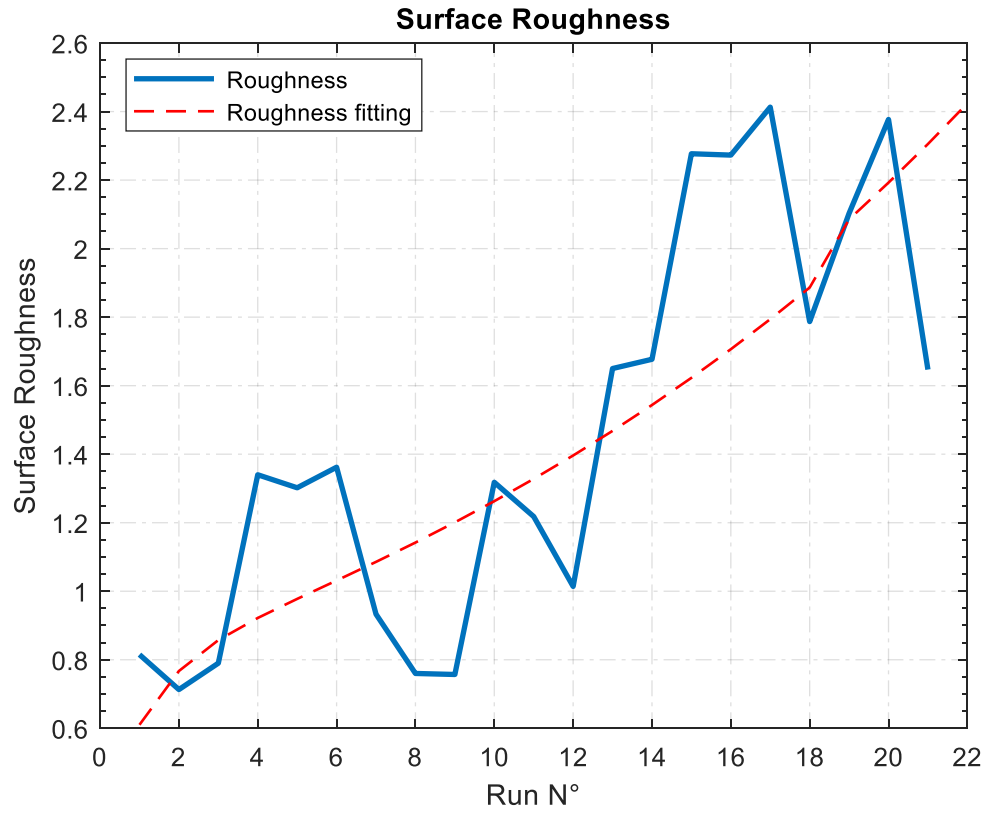

Fig. 12 Surface Roughness variation over the twenty-one runs

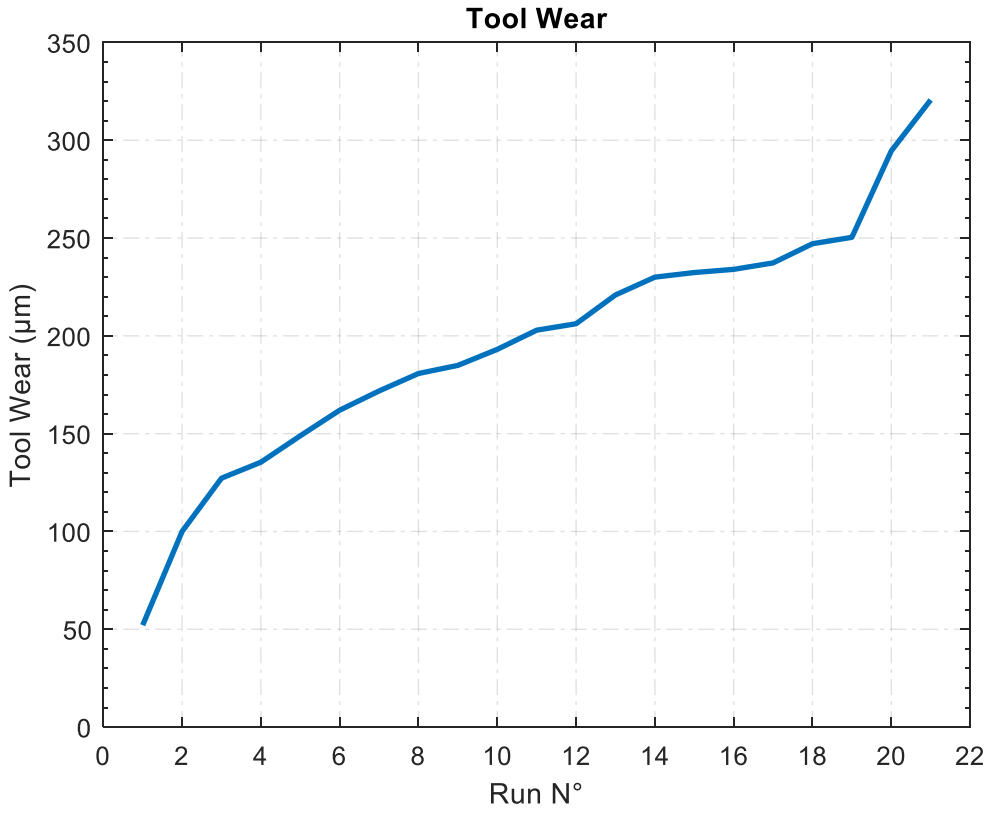

Fig. 13 Flank wear variation over the Twenty-one runs

Acknowledgment

The machines, devices and tools used in this work, are the property of the Mechanics Research Center of Constantine, the latter is financed by the Algerian Ministry of Higher education and Scientific Research.

References

[1] D. E. Dimla, The Correlation of Vibration Signal Features to Cutting Tool Wear in a Metal Turning Operation, Int. J. Adv. Manuf. Technol., vol. 19, no. 10, pp. 705–713, Jun.2002.

[2] Niu, B., Sun, J., & Yang, B. (2020). Multisensory based tool wear monitoring for practical applications in milling of titanium alloy. Materials Today: Proceedings, 22, 1209-1217.

[3] Chen, N., Hao, B., Guo, Y., Li, L., Khan, M. A., & He, N. (2020). Research on tool wear monitoring in drilling process based on APSO-LS-SVM approach. The International Journal of Advanced Manufacturing Technology, 108, 2091-2101.

[4] Zhang, X., Han, C., Luo, M., & Zhang, D. (2020). Tool Wear Monitoring for Complex Part Milling Based on Deep Learning. Applied Sciences, 10(19), 6916.

[5] Inţă, M., & Muntean, A. (2018). Researches regarding introducing temperature as a factor in cutting tool wear monitoring. In *MATEC Web of Conferences* (Vol. 178, p. 01013). EDP Sciences.

[6] Thirukkumaran, K., Menaka, M., Mukhopadhyay, C. K., & Venkatraman, B. (2020). A study on temperature rise, tool Wear, and surface roughness during Drilling of Al–5% SiC composite. Arabian Journal for Science and Engineering, 45(7), 5407-5419.

[7] Tamerabet, Y., Brioua, M., Tamerabet, M., & Khoualdi, S. (2018). Experimental Investigation on Tool Wear Behavior and Cutting Temperature during Dry Machining of Carbon Steel SAE 1030 Using KC810 and KC910 Coated Inserts. Tribology in Industry, 40(1).

[8] Özbek, O., & Saruhan, H. (2020). The effect of vibration and cutting zone temperature on surface roughness and tool wear in eco-friendly MQL turning of AISI D2. *Journal of Materials Research and Technology*, *9*(3), 2762-2772.

[9] Angelone, R., Caggiano, A., Improta, I., Nele, L., & Teti, R. (2018). Temperature measurements for the tool wear and hole quality assessment during drilling of CFRP/CFRP stacks. *Procedia CIRP*, *67*, 416-421.

[10] Da Silva, L. R. R., Del Claro, V. T. S., Andrade, C. L. F., Guesser, W. L., Jackson, M. J., & Machado, A. R. (2021). Tool wear monitoring in drilling of high-strength compacted graphite cast irons. *Proceedings of the Institution of Mechanical Engineers, Part B: Journal of Engineering Manufacture*, *235*(1-2), 207-218.

[11] Oo, H., Wang, W., & Liu, Z. (2020). Tool wear monitoring system in belt grinding based on image-processing techniques. *The International Journal of Advanced Manufacturing Technology*, *111*(7), 2215-2229.

[12] Li, Z., Liu, R., & Wu, D. (2019). Data-driven smart manufacturing: tool wear monitoring with audio signals and machine learning. *Journal of Manufacturing Processes*, *48*, 66-76.

[13] Dou, J., Xu, C., Jiao, S., Li, B., Zhang, J., & Xu, X. (2020). An unsupervised online monitoring method for tool wear using a sparse auto-encoder. *The International Journal of Advanced Manufacturing Technology*, *106*(5), 2493-2507.

[14] Kiew, C. L., Brahmananda, A., Islam, K. T., Lee, H. N., Venier, S. A., Saraar, A., & Namazi, H. (2020). Complexity-based analysis of the relation between tool wear and machine vibration in turning operation. Fractals, 28(01), 2050018.

[15] Móricz, L., Viharos, Z. J., Németh, A., Szépligeti, A., & Büki, M. (2020). Off-line geometrical and microscopic & on-line vibration based cutting tool wear analysis for micro-milling of ceramics. Measurement, 163, 108025.

[16] Babouri, M. K., Ouelaa, N., Djamaa, M. C., Djebala, A., & Hamzaoui, N. (2017). Prediction of tool wear in the turning process using the spectral center of gravity. Journal of Failure Analysis and Prevention, 17(5), 905-913.

[17] Stavropoulos, P., Papacharalampopoulos, A., & Souflas, T. (2020). Indirect online tool wear monitoring and model-based identification of process-related signal. Advances in Mechanical Engineering, 12(5), 1687814020919209.

[18] Marani, M., Zeinali, M., Kouam, J., Songmene, V., & Mechefske, C. K. (2020). Prediction of cutting tool wear during a turning process using artificial intelligence techniques. The International Journal of Advanced Manufacturing Technology, 111(1), 505-515.

[19] Lauro, C. H., Brandão, L. C., Baldo, D., Reis, R. A., & Davim, J. P. (2014). Monitoring and processing signal applied in machining processes–A review. Measurement, 58, 73-86.

[20] Mali, R., Telsang, M. T., & Gupta, T. V. K. (2017). Real time tool wear condition monitoring in hard turning of Inconel 718 using sensor fusion system. Materials Today: Proceedings, 4(8), 8605-8612.

[21] Yang, Z., & Yu, Z. (2012). Grinding wheel wear monitoring based on wavelet analysis and support vector machine. The International Journal of Advanced Manufacturing Technology, 62(1), 107-121.

[22] Choi, Y., Narayanaswami, R., & Chandra, A. (2004). Tool wear monitoring in ramp cuts in end milling using the wavelet transform. The International Journal of Advanced Manufacturing Technology, 23(5), 419-428.

[23] Cao, X., Chen, B., Yao, B., & Zhuang, S. (2019). An intelligent milling tool wear monitoring methodology based on convolutional neural network with derived wavelet frames coefficient. Applied Sciences, 9(18), 3912.

[24] Patra, K., Pal, S. K., & Bhattacharyya, K. (2007). Application of wavelet packet analysis in drill wear monitoring. Machining Science and Technology, 11(3), 413-432.

[25] KHEMISSI, B. M., Ouelaa, N., & Djebala, A. (2017). Application of the empirical mode decomposition method for the prediction of the tool wear in turning operation. Mechanics, 23(2), 315-320.

[26] Wolszczak, P., Łygas, K., & Litak, G. (2017). Monitoring of cutting conditions with the empirical mode decomposition. Advances in Science and Technology Research Journal, 11.

[27] Raja, J. E., Kiong, L. C., & Soong, L. W. (2013). Hilbert–Huang transform-based emitted sound signal analysis for tool flank wear monitoring. Arabian Journal for Science and Engineering, 38(8), 2219-2226.

[28] Babouri, M. K., Ouelaa, N., Djebala, A., Djamaa, M. C., & Boucherit, S. (2017). Prediction of cutting tool's optimal lifespan based on the scalar indicators and the wavelet multi-resolution analysis. In Applied Mechanics, Behavior of Materials, and Engineering Systems (pp. 299-310). Springer, Cham.

[29] Xu, C., Chai, Y., Li, H., & Shi, Z. (2018). Estimation the wear state of milling tools using a combined ensemble empirical mode decomposition and support vector machine method. Journal of Advanced Mechanical Design, Systems, and Manufacturing, 12(2), JAMDSM0059-JAMDSM0059.

[30] Wang, T., Zhang, M., Yu, Q., & Zhang, H. (2012). Comparing the applications of EMD and EEMD on time–frequency analysis of seismic signal. Journal of Applied Geophysics, 83, 29-34.

[31] Shrivastava, Y., & Singh, B. (2019). A comparative study of EMD and EEMD approaches for identifying chatter frequency in CNC turning. European Journal of Mechanics-A/Solids, 73, 381-393.

[32] Wu, Z., & Huang, N. E. (2009). Ensemble empirical mode decomposition: a noise-assisted data analysis method. Advances in adaptive data analysis, 1(01), 1-41.

[33] Jenitta, J., & Rajeswari, A. (2013, April). Denoising of ECG signal based on improved adaptive filter with EMD and EEMD. In 2013 IEEE Conference on Information & Communication Technologies (pp. 957-962). IEEE.

[34] Bouhalais, M. L., Djebala, A., Ouelaa, N., & Babouri, M. K. (2018). CEEMDAN and OWMRA as a hybrid method for rolling bearing fault diagnosis under variable speed. The International Journal of Advanced Manufacturing Technology, 94(5), 2475-2489.

[35] Colominas, M. A., Schlotthauer, G., & Torres, M. E. (2014). Improved complete ensemble EMD: A suitable tool for biomedical signal processing. Biomedical Signal Processing and Control, 14, 19-29.

Declarations

Funding: The work is financed by the Algerian Ministry of Higher education and Scientific Research.

Conflicts of interest/Competing interests: I, Doctor Moahamed Lamine BOUHALAIS, corresponding author of the paper, certify that we have no potential conflict of interest for the presented article

Availability of data and material: Not applicable

Code availability: Not applicable

Authors' contributions: (optional)

Additional declarations for articles in life science journals that report the results of studies involving humans and/or animals: Not applicable

Ethics approval: I certify that the paper follows the ethical rules of good scientific practice mentioned in the “Ethical Responsibilities of Authors” of the journal.

Consent to participate Not applicable

Consent for publication Author hereby grants to Springer International Publishing the right to publish this work.

Figures

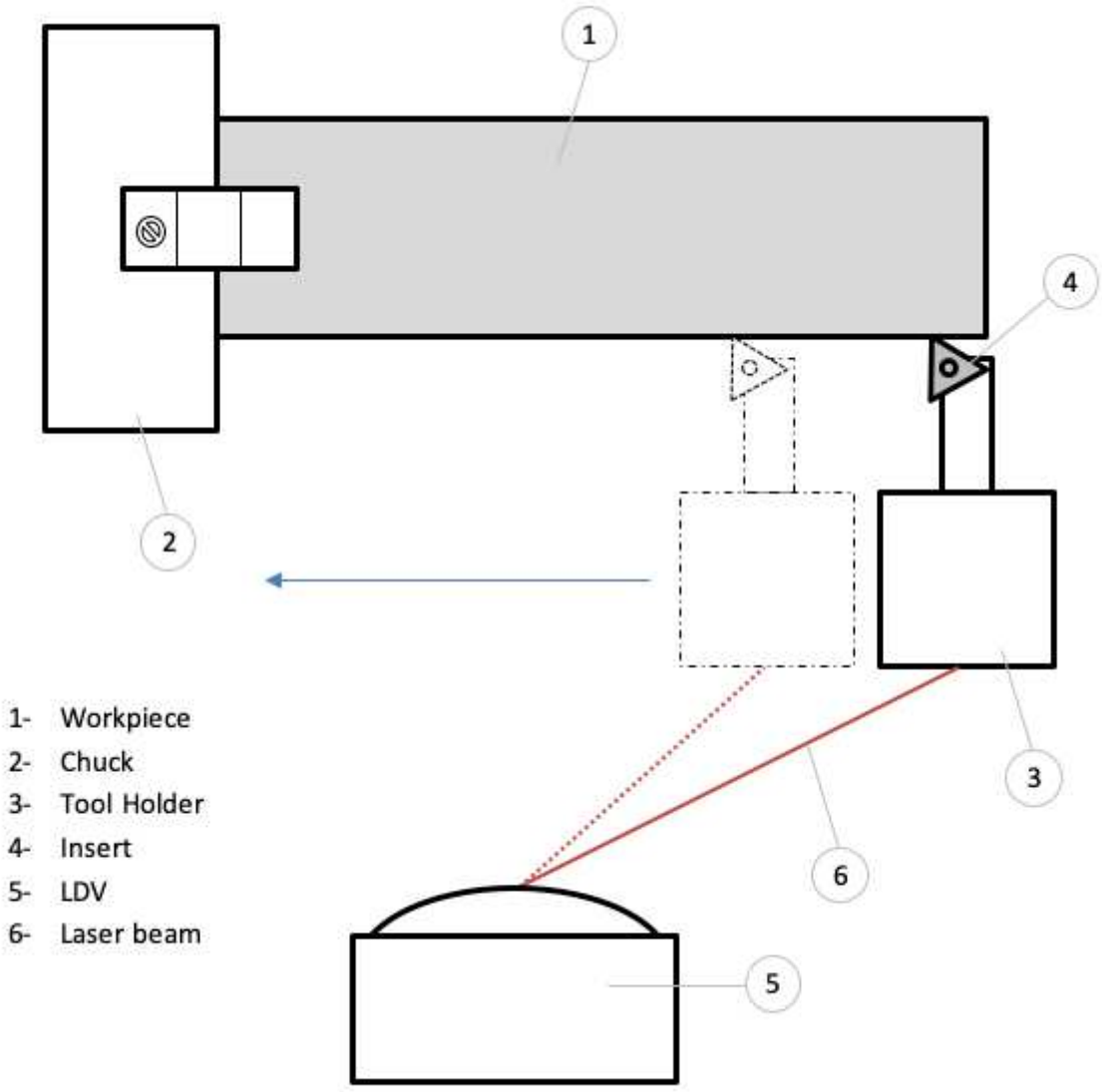

Figure 1

The experimental setup

Figure 2

The used equipments

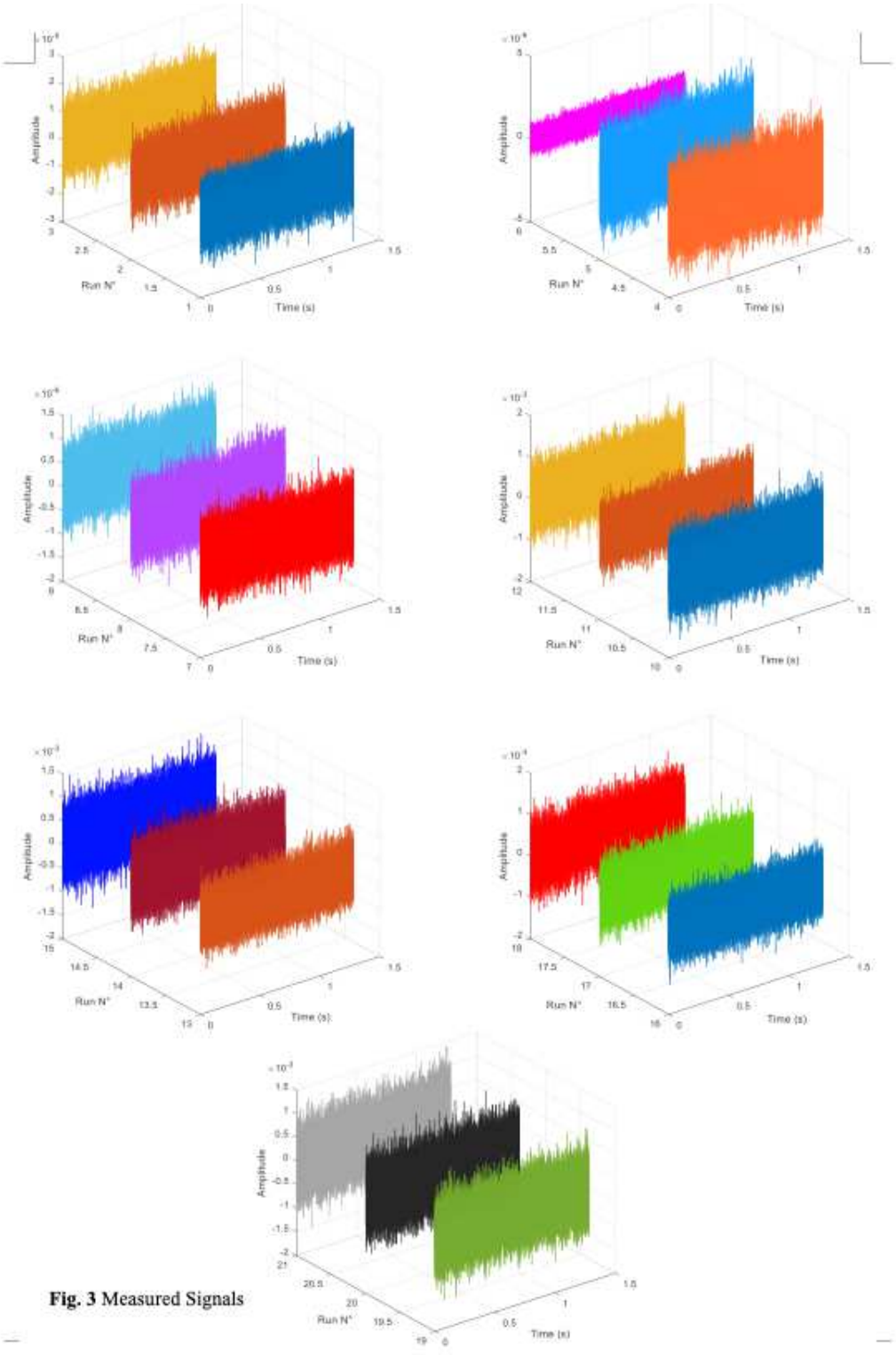

Fig. 3 Measured Signals

Figure 3

Measured Signals

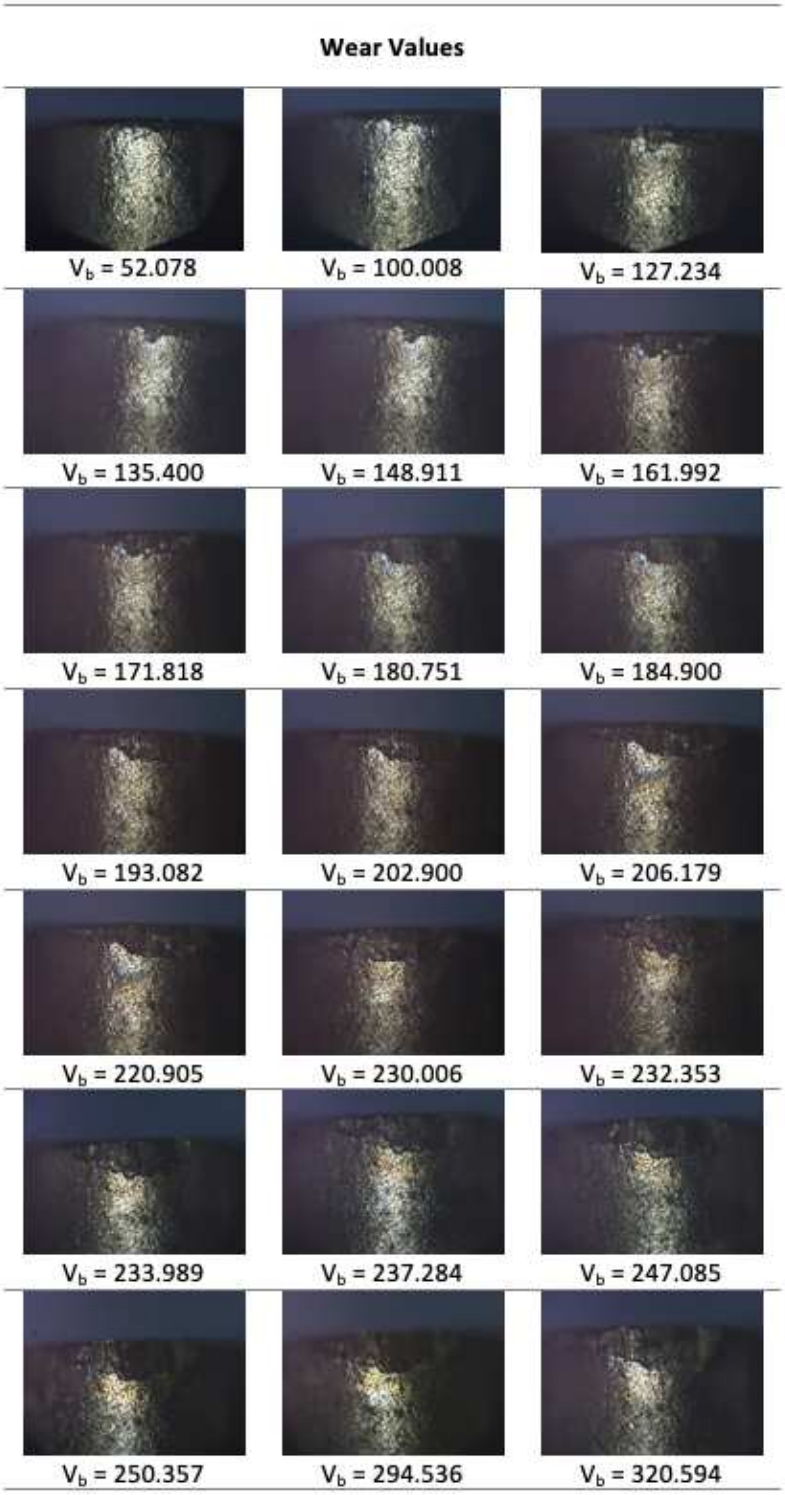

Figure 4

Flank wear progression as shown by the microscope

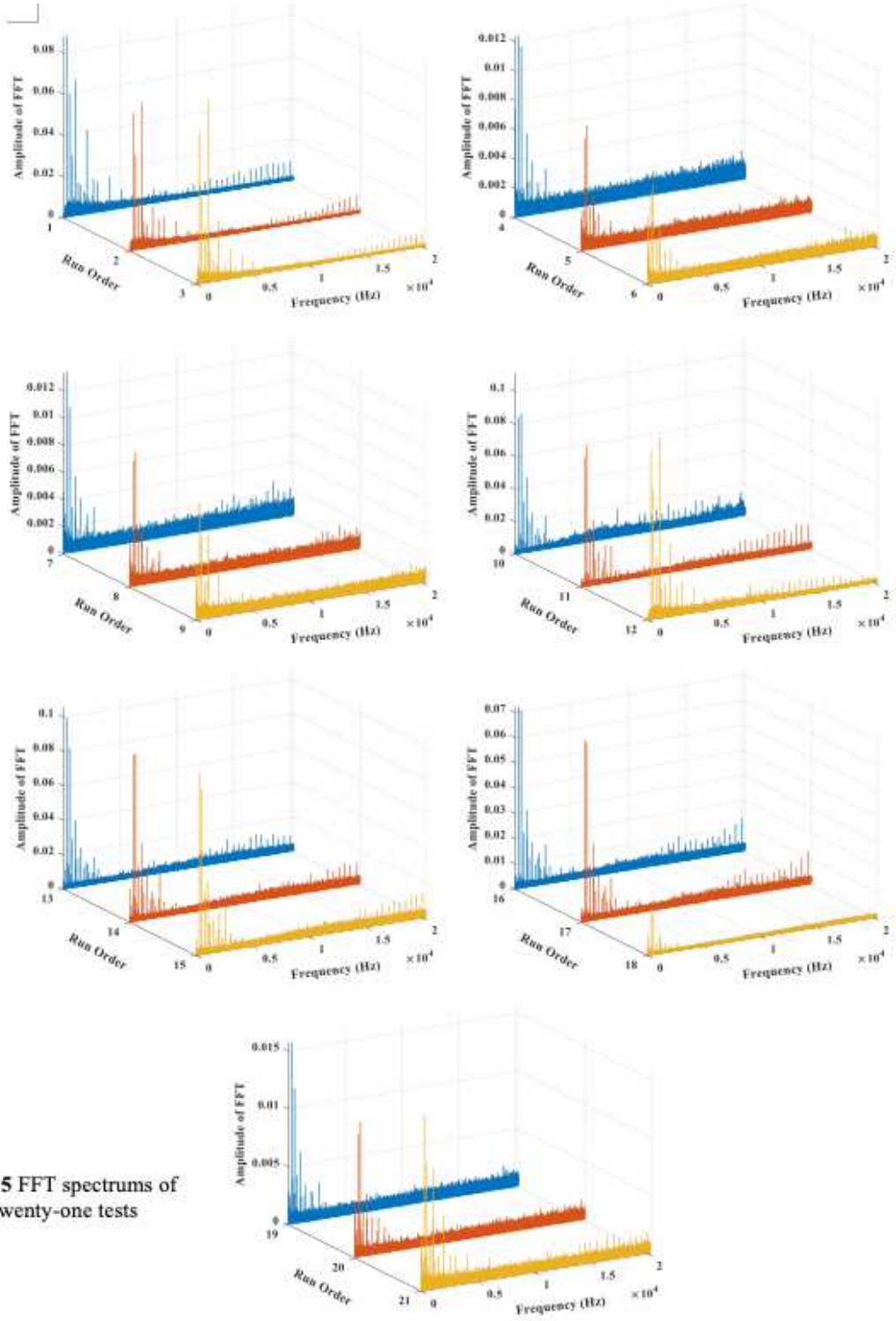

Fig. 5 FFT spectrums of the twenty-one tests

Figure 5

FFT spectrums of the twenty-one tests

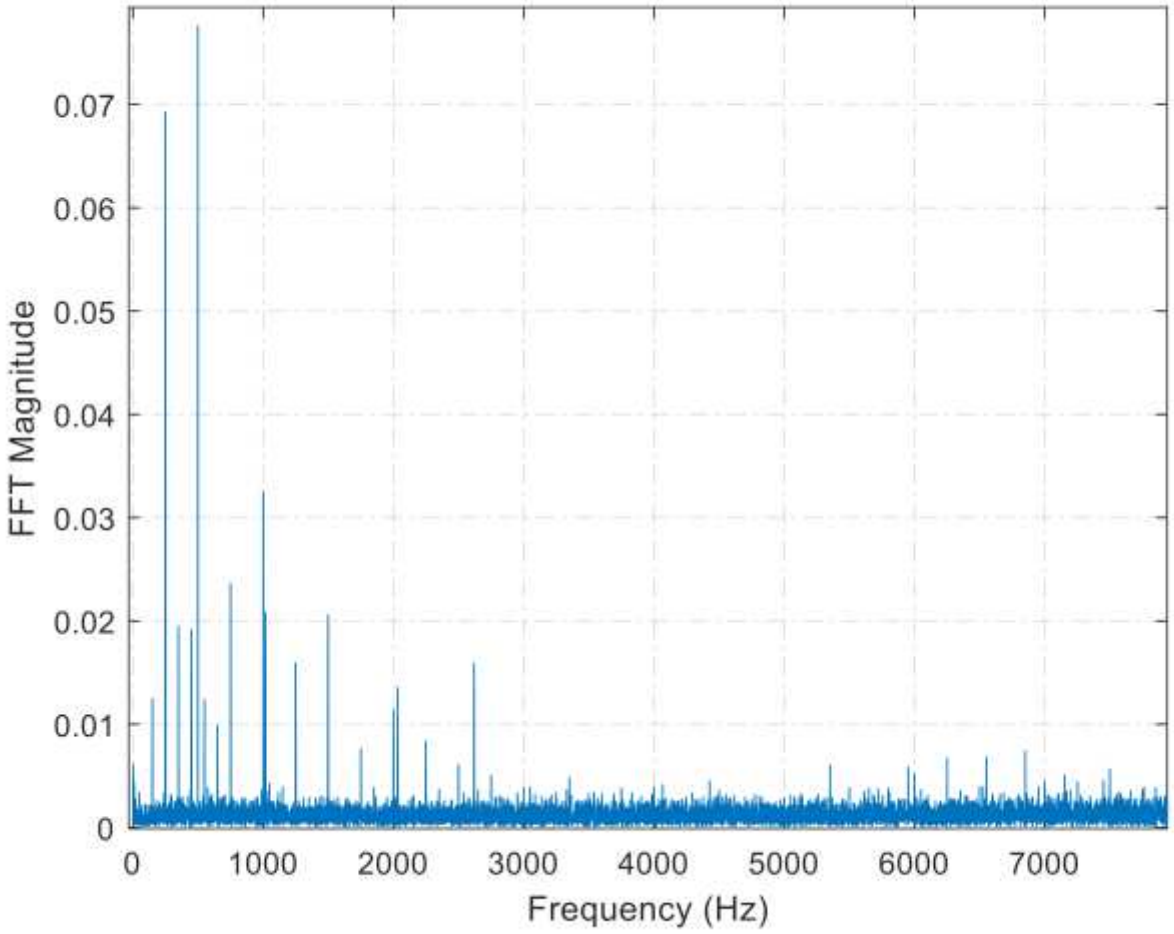

Figure 6

Contactless Test signal spectrum

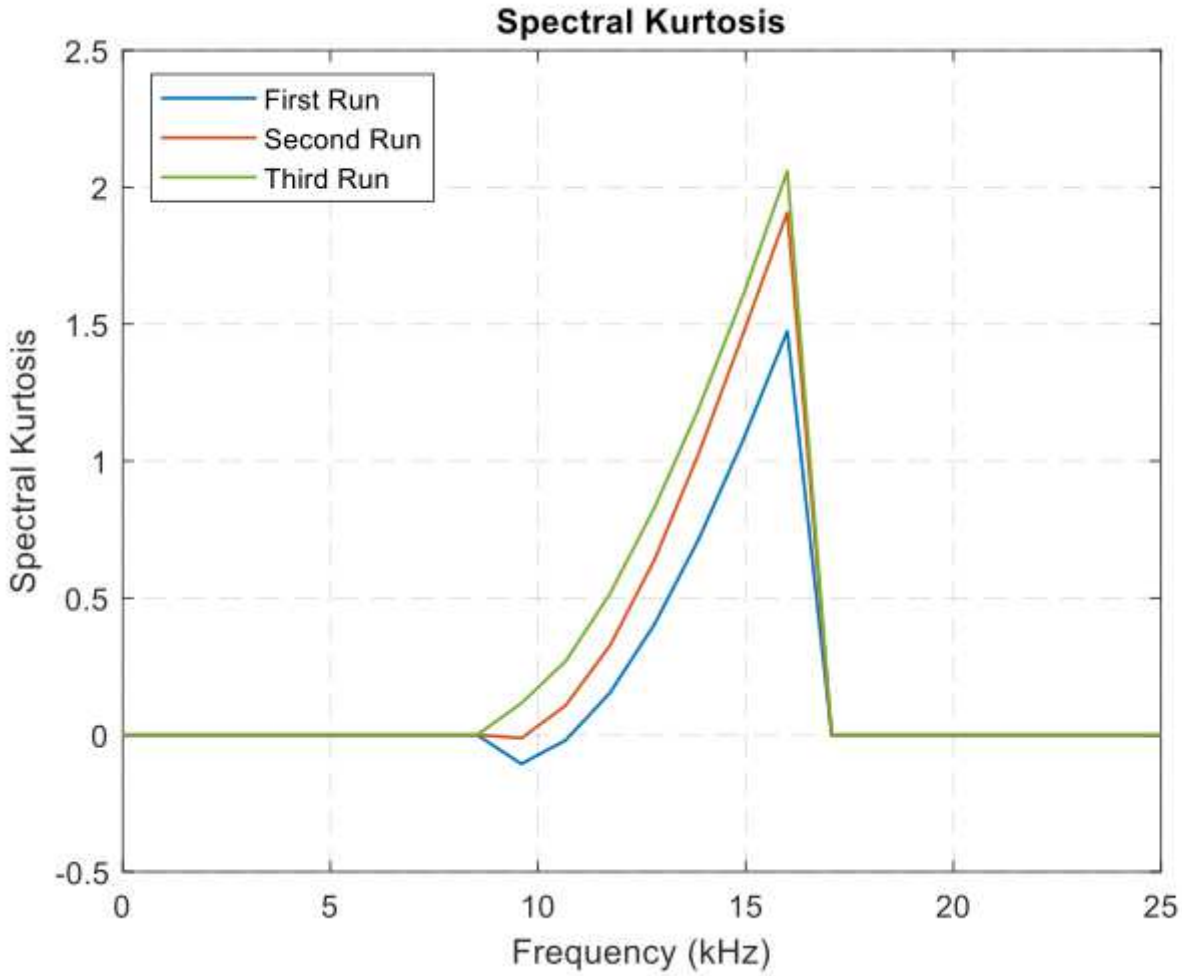

Figure 7

SK of the first three runs signals

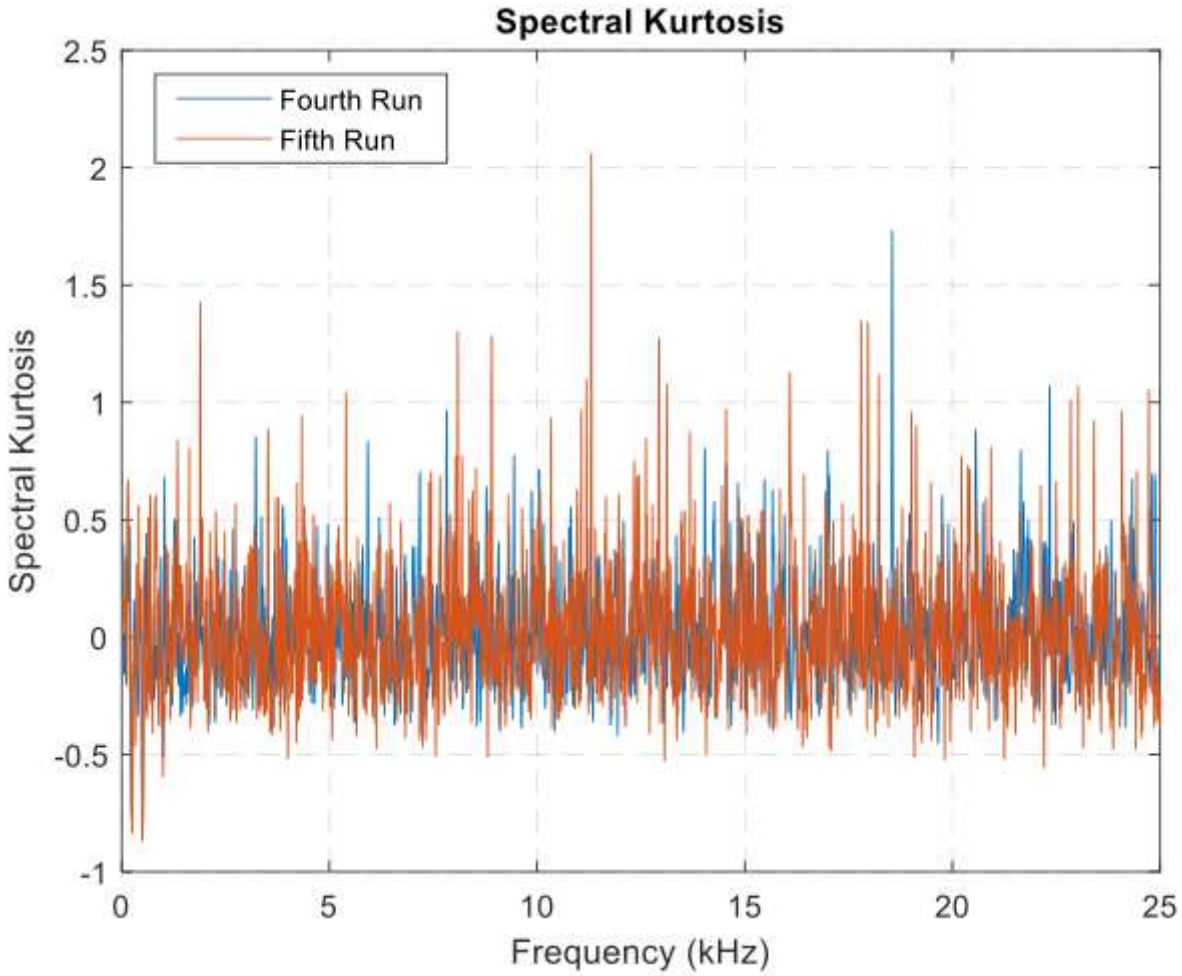

Figure 8

Spectral Kurtosis of the Fourth and Fifth runs signals

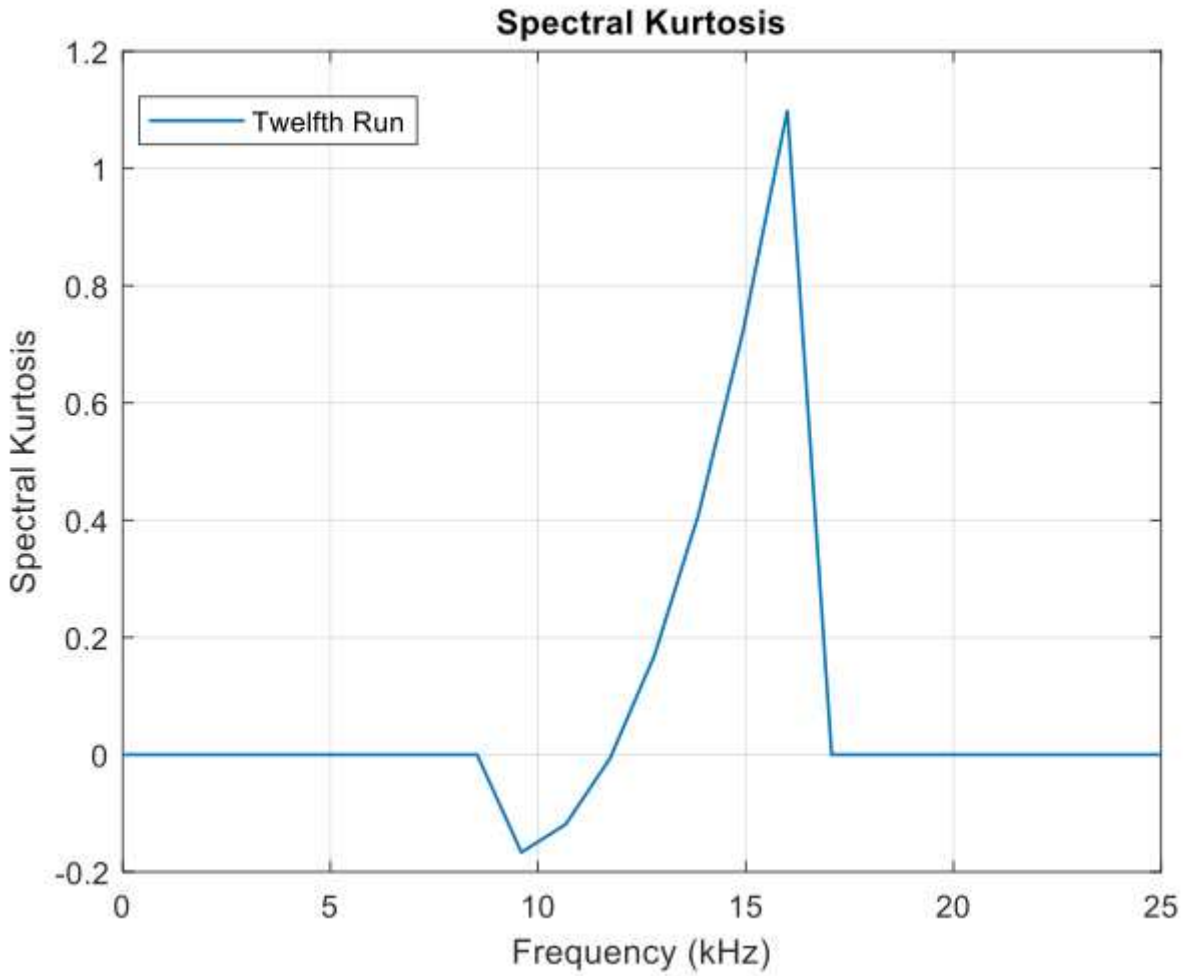

Figure 9

Spectral Kurtosis of the Twelfth run signal

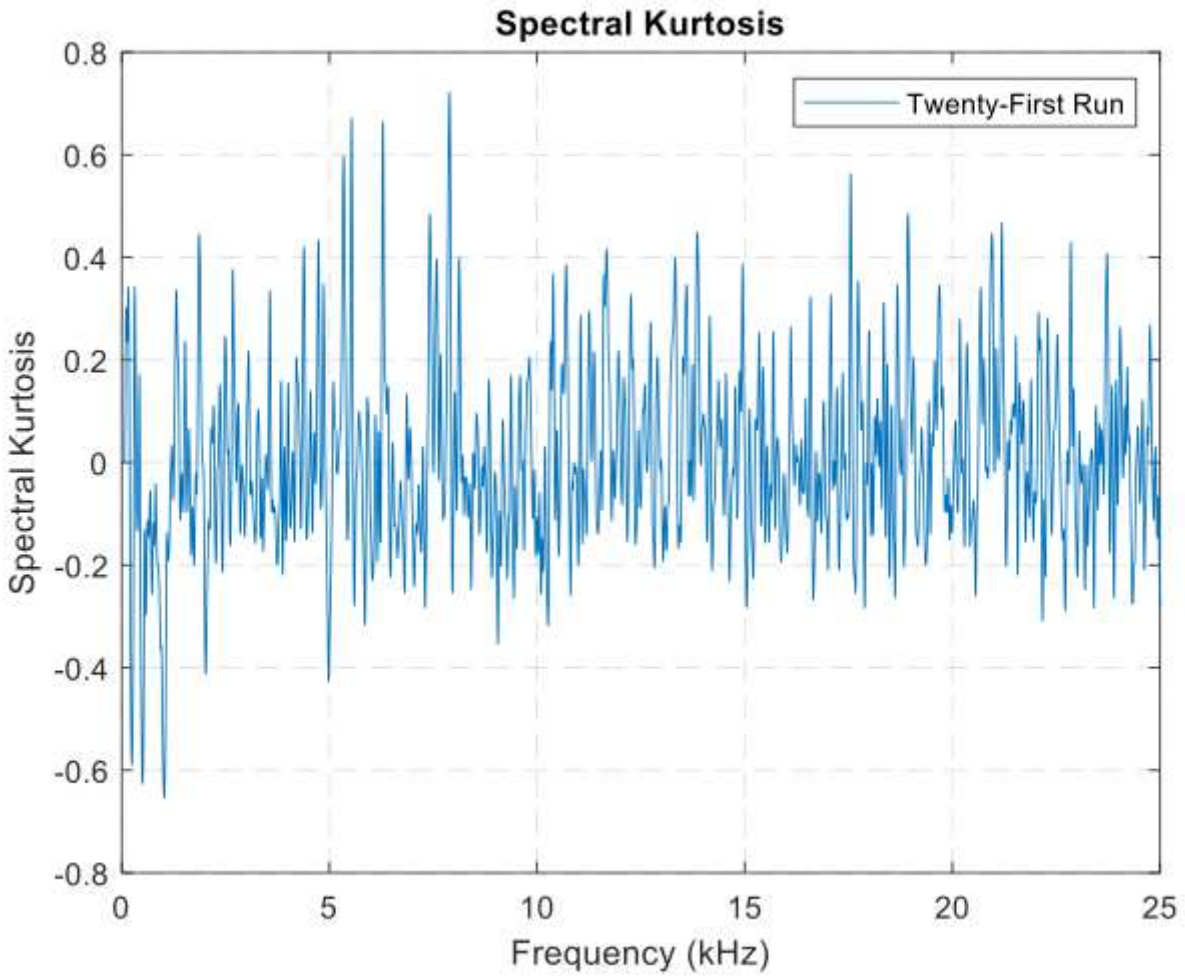

Figure 10

Spectral Kurtosis of the Twenty-first run signal

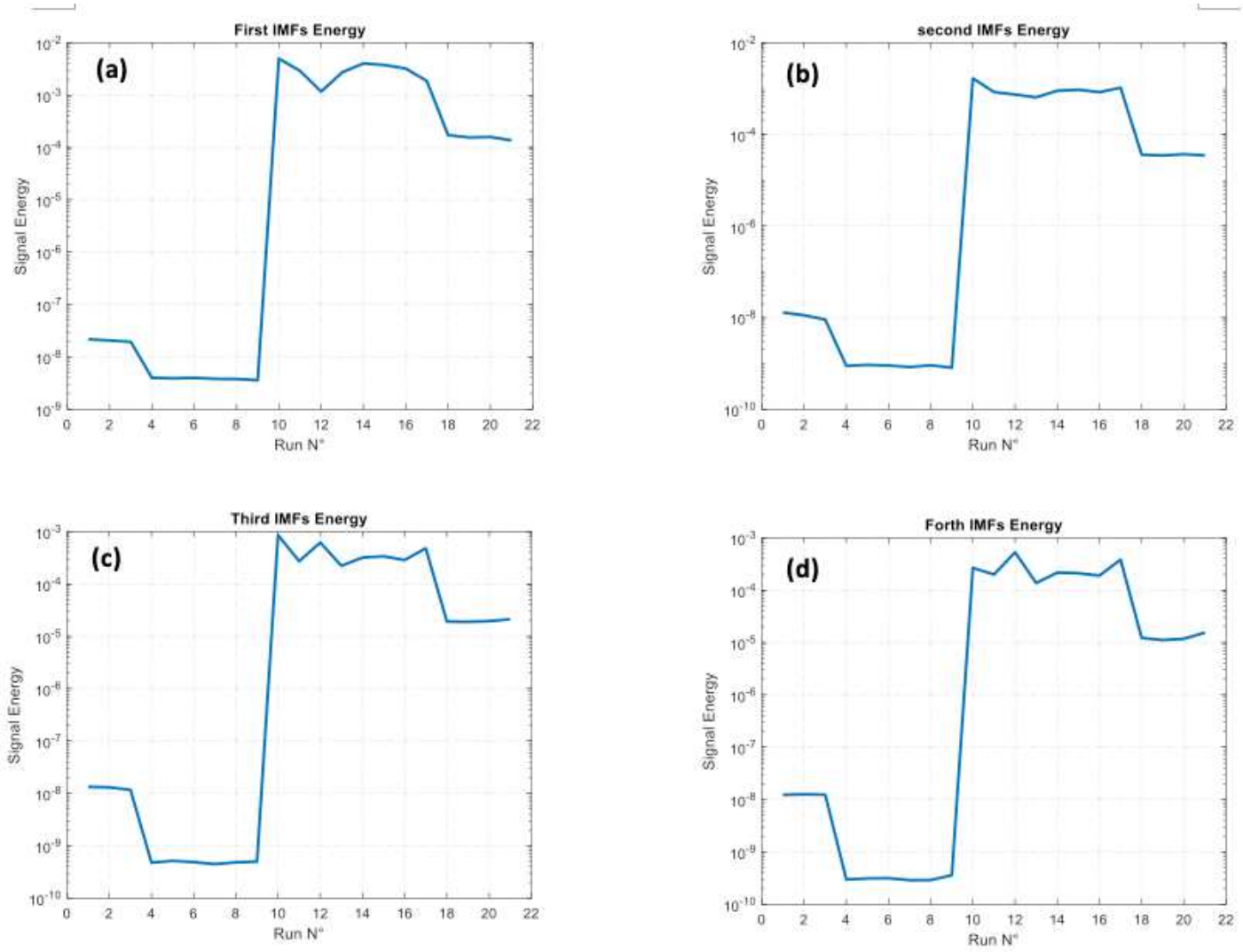

Figure 11

IMF Energy variation over the twenty-one runs: Firsts (a), Seconds (b), Thirds (c) and Fourths (d)

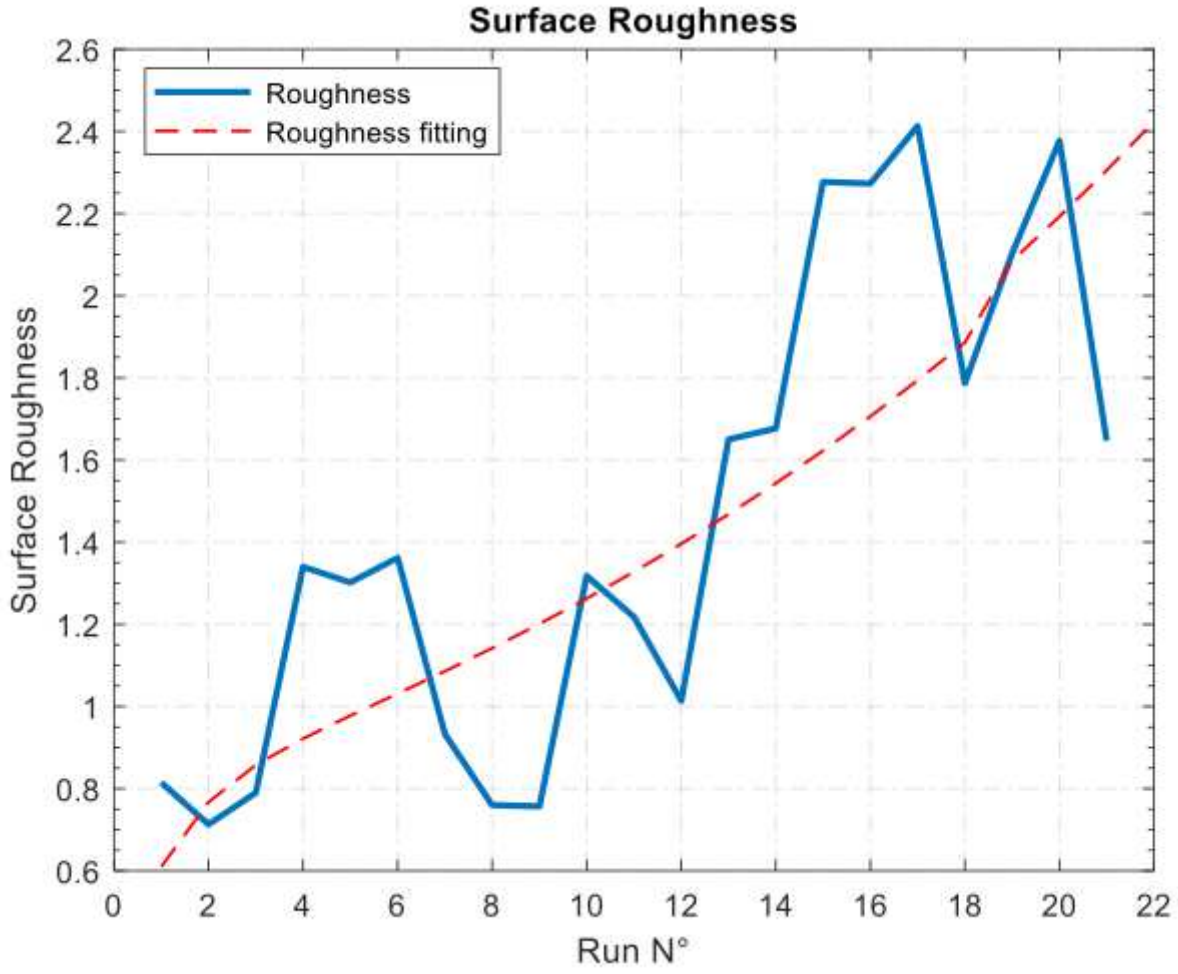

Figure 12

Surface Roughness variation over the twenty-one runs

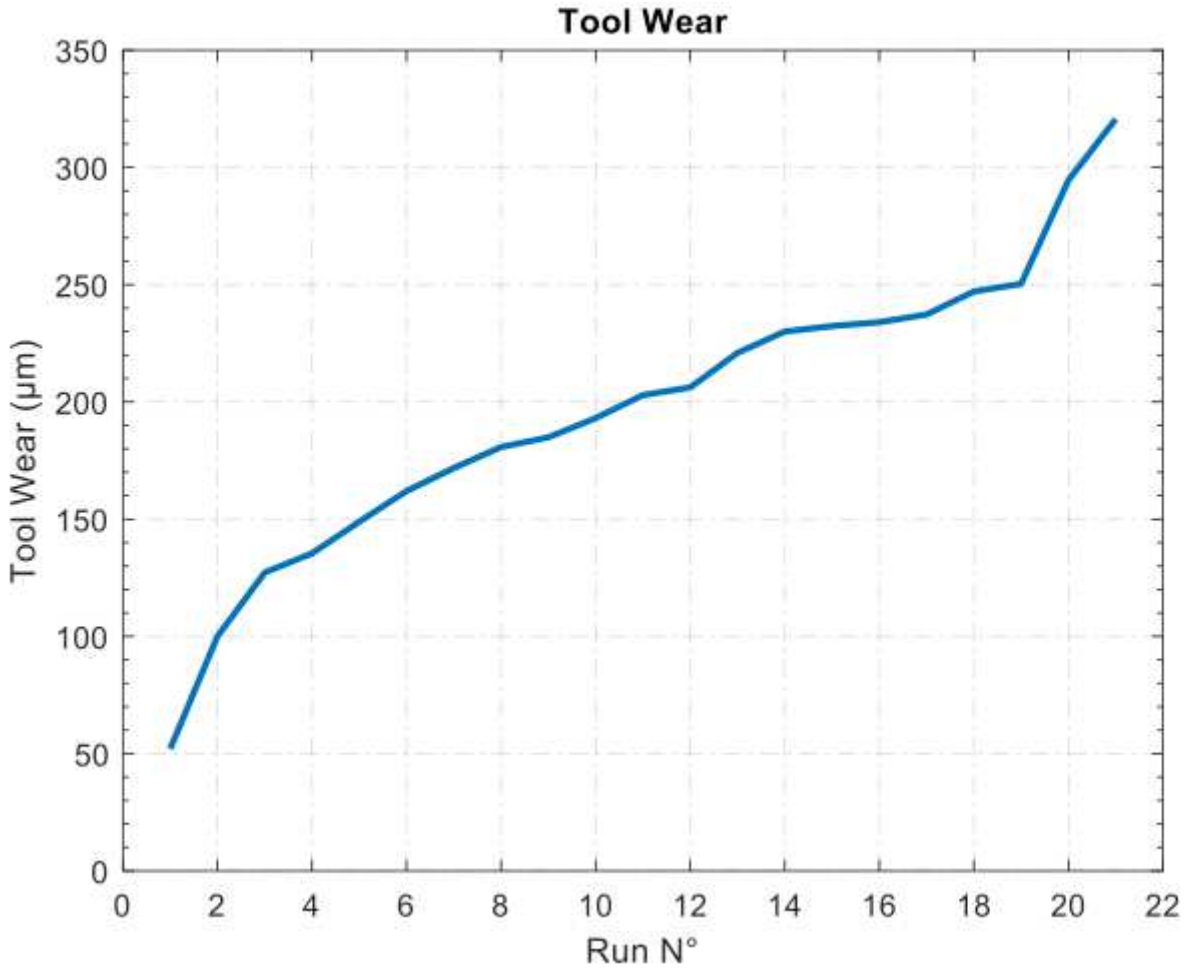

Figure 13

Flank wear variation over the Twenty-one runs